Contents lists available at AccScience Publishing
Nonlinear Science and Control Engineering (NSCE)
Vol. 2, No. 1 (2026)
https://accscience.com/journal/nsce

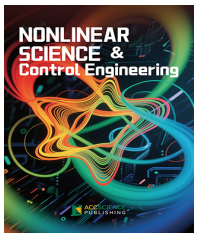

Memristor-coupled tabu learning neuron and multi-cavity control of attractors

Xiyu Ren[1], Xianying Xu[1]*, Xiaodong Liu[2]*, Yinghong Cao[1], Suo Gao[1], and Jun Mou[1]

[1]*School of Information Science and Engineering, Dalian Polytechnic University, Dalian, Liaoning, China*
[2]*School of Innovation and Entrepreneurship, Dalian Polytechnic University, Dalian, Liaoning, China*

Article History:
Received: September 30, 2025
Revised: October 20, 2025
Accepted: November 3, 2025
Published online: December 9, 2025

ABSTRACT

The tabu learning neuron model is constructed by coupling the tabu search algorithm with a neural network model designed to simulate the electrical activity and synchronous behavior of biological neural systems. This paper proposes a self-coupled tabu learning neuron-memristor (TLNM) system by integrating a tabu learning neuron with a newly proposed universal magnetically controlled memristor. The dynamical characteristics of the TLNM system were analyzed by plotting the Lyapunov exponent spectrum, bifurcation diagram, attractors, and spectral entropy complexity. During this process, it was found that the TLNM system exhibited a wide range of firing behaviors. Multi-cavity control of attractors generated by the TLNM system was achieved by introducing a multi-level step-function approach. Finally, the physical feasibility of the TLNM system was verified on the demand-side platform. The TLNM system proposed in this paper provides a theoretical foundation for studying brain-like behavior.

Keywords: Tabu learning neuron; Tabu learning neuron-memristor; Dynamical characteristics; Demand-side platform

CC BY

1. Introduction

The brain is the most important part of the nervous system.[1] It contains a diverse array of neuron types, and it is through the collective action of these neurons that humans are able to perform various behaviors.[2] Research on the human brain has revealed its nonlinear behavior, which bears similarities to the chaos theory.[3,4] The profound insight of chaos theory lies in the fact that simple deterministic systems can also produce extremely complex and quasi-random behavior. Therefore, researchers have applied chaos theory to the study of the human brain and have constructed numerous chaotic neural network models.[5,6] These neural network models exhibit rich dynamic properties, providing a more realistic computational framework for simulating the brain's memory, association, and decision-making processes. In 1952, the Hodgkin–Huxley model laid the foundation for computational neuroscience by precisely describing ion channel dynamics[7], but its complex differential equations hindered large-scale network simulations. Subsequently,

***Corresponding authors**:
Xianying Xu (xuxiany@dlpu.edu.cn).
Xiaodong Liu (liuxiaod@dlpu.edu.cn).

Citation: Ren X, Xu X, Liu X, Cao Y, Gao S, Mou J. Memristor-coupled tabu learning neuron and multi-cavity control of attractors. *Nonlinear Sci Cont Eng.* 2026;2(1):025400014. doi: 10.36922/NSCE025400014

Copyright: © 2025 The Author(s). This is an Open Access article distributed under the terms of the Creative Commons Attribution License, permitting distribution, and reproduction in any medium, provided the original work is properly cited.

proposed simplified models, such as the Hindmarsh–Rose model, while preserving rich discharge patterns, clearly revealed the chaotic dynamics of neuronal activity, providing key insights into the study of chaotic neural networks.[8,9] However, when these models, which are based on continuous dynamics, are applied to optimization computations, they often face the challenge of effectively controlling and utilizing chaos. To address this challenge, the tabu neuron model is developed.[10,11] This model innovatively incorporates a tabu mechanism that simulates the refractory period of biological neurons: after excitation, a neuron enters a brief self-inhibitory state during which its excitability is significantly reduced. Tabu neurons possess self-regulatory capabilities, enabling networks that are based on them to be directly and efficiently applied to complex computational tasks, such as combinatorial optimization (e.g., the traveling salesman problem) and associative memory, without requiring intricate external parameter control.

When constructing neural networks, traditional complementary metal-oxide-semiconductor-based synapse circuits face inherent bottlenecks in integration density, power consumption, and plasticity. To overcome these limitations and better simulate the parallel, adaptive, and integrated information storage processing mechanisms found in biological brains, memristors—as an emerging class of nanoscale electronic devices—have been regarded in recent years as ideal candidates for realizing electronic synapses.[12–15] In 1971, Chua[16] proposed the memristor, a unique component capable of recording the amount of charge that flows through it. Consequently, memristors are widely employed in various fields, such as information storage and electronic synapses. More importantly, the memristor itself typically exhibits rich nonlinear dynamic properties.[17,18] This makes the synapse constructed from memristors not only a variable connection weight, but also potentially an additional nonlinear dynamical system in its own right. Therefore, memristor has gradually gained attention among researchers.[19–22] Combining memristors as electronic synapses with chaotic neuron models holds significant research value.[23–25] In 2024, Yang *et al.*[26] provided actionable guidance for the practical application of memristor systems. They summarized field coupling between memristor systems, electromagnetic induction, and radiation phenomena in cardiac tissue, as well as the application of memristor systems in image encryption. In 2023, Lai and Yang[27] constructed three discrete neural network models and discovered that a discrete memristor could induce more complex chaotic dynamics in neural network models. In 2024, Yu *et al.*[28] proposed a non-polynomial memristor that integrates adaptive sliding mode control methods to construct a novel adaptive synchronization scheme for simulating neural network synchronization. Therefore, it is essential to investigate the integration of memristors as electronic synapses with chaotic neuron models.[29–31]

In recent years, researchers have increasingly focused on coupling the memristors with neural network models.[32] In 2024, Mou *et al.*[33] designed a locally active memristor and applied it to couple FitzHugh–Nagumo and Hindmarsh–Rose neurons, simulating the coupling and information transmission mechanisms between different neurons. In 2023, Lin *et al.*[34] coupled a memristor with two asymmetric neural networks to construct the memory-augmented neural network model, analyzed its dynamic properties, and applied it to the secure communications field. In 2024, Zhang *et al.*[35] proposed a network of morphologically memristor-coupled adaptive synaptic neurons and investigated its fully synchronized and delayed synchronized phenomena through numerical analysis.

The current study proposes a self-coupled universal magnetically controlled memristor with a tabu learning neuron and constructs the tabu learning neuron-memristor (TLNM) model. The tabu learning neuron inherently exhibits complex dynamic properties. Upon incorporating the nonlinear memristor element, its dynamic behavior becomes even more diverse and tunable. This offers a highly promising technical pathway for constructing next-generation neuromorphic computers with exceptional energy efficiency and biological realism. The remainder of this paper is structured as follows: Section 2 presents the analysis of the characteristics of the proposed universal magnetically controlled memristor. Section 3 describes the establishment process of the TLNM system and analyzes its stability. In Section 4, the TLNM system is investigated using numerical analysis methods, and its multi-cavity attractor is controlled. In Section 5, the attractor obtained from the TLNM system simulation is implemented via the Demand-side platform (DSP). Finally, Section 6 concludes the findings of this study.

2. Electronic synapse

The tanh function exhibits smooth, differentiable, and symmetric soft saturation characteristics. This makes it an ideal mathematical model for simulating real-world nonlinear phenomena. This paper proposes a novel universal magnetically controlled memristor based on the tanh function to serve as an electronic synapse connecting neurons. The mathematical model of this universal magnetically controlled memristor is shown in Equation (1). Where $W(\varphi_n)$ denotes the memristor's memristance, φ_n represents the flux state variable, and v_n is the memristor excitation voltage. The structure of this universal magnetically controlled memristor is shown in Figure 1.

$$\begin{cases} i_n = W(\varphi_n)\, v_n \\ W(\varphi_n) = \tanh^3 \varphi_n + \tanh \varphi_n \\ \varphi_{n+1} = a \tanh\left(\varphi_n^2 + \varphi_n\right) + b v_n \end{cases} \tag{1}$$

The feasibility of memristors can be verified by plotting their pinched hysteresis loops. The pinched hysteresis loops of the memristor form an "8" shape. As the frequency of the excitation voltage applied across the memristor increases, the area of the pinched hysteresis loops gradually decreases. At high frequencies, the pinched hysteresis loops approach a straight line. As the amplitude of the excitation voltage that is applied across the memristor increases, the area of the pinched hysteresis loops gradually expands. The pinched hysteresis loops of the memristor proposed in this paper are shown in Figure 2. The pinched hysteresis loops as a function of frequency are shown in Figure 2A. The pinched hysteresis loops with amplitude variation are shown in Figure 2B.

3. The tabu learning neuron-memristor model

3.1. The development of the tabu learning neuron-memristor model

The discrete tabu learning neuron model is constructed by coupling the tabu search algorithm with neural models,

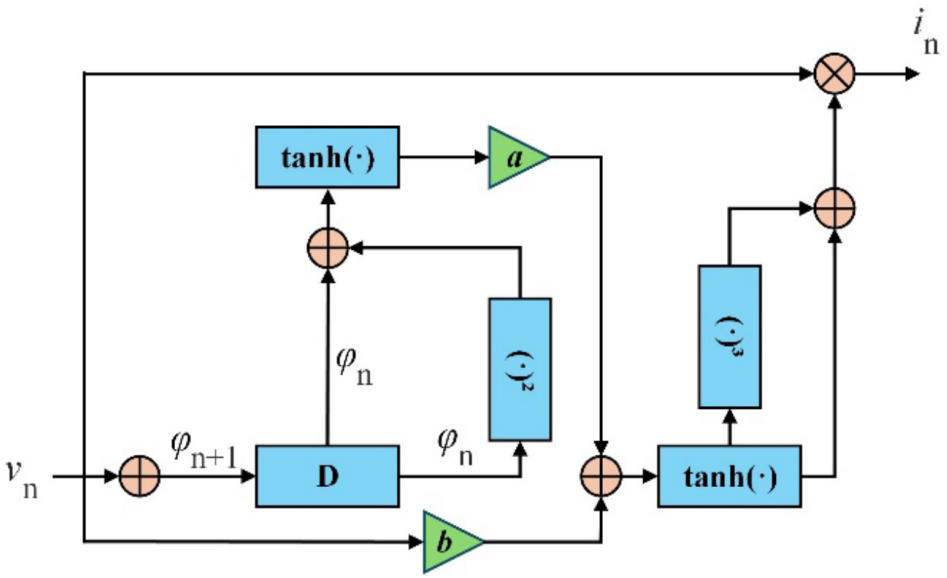

Figure 1. Schematic diagram of a universal magnetically controlled memristor
Abbreviation: D: Delay element.

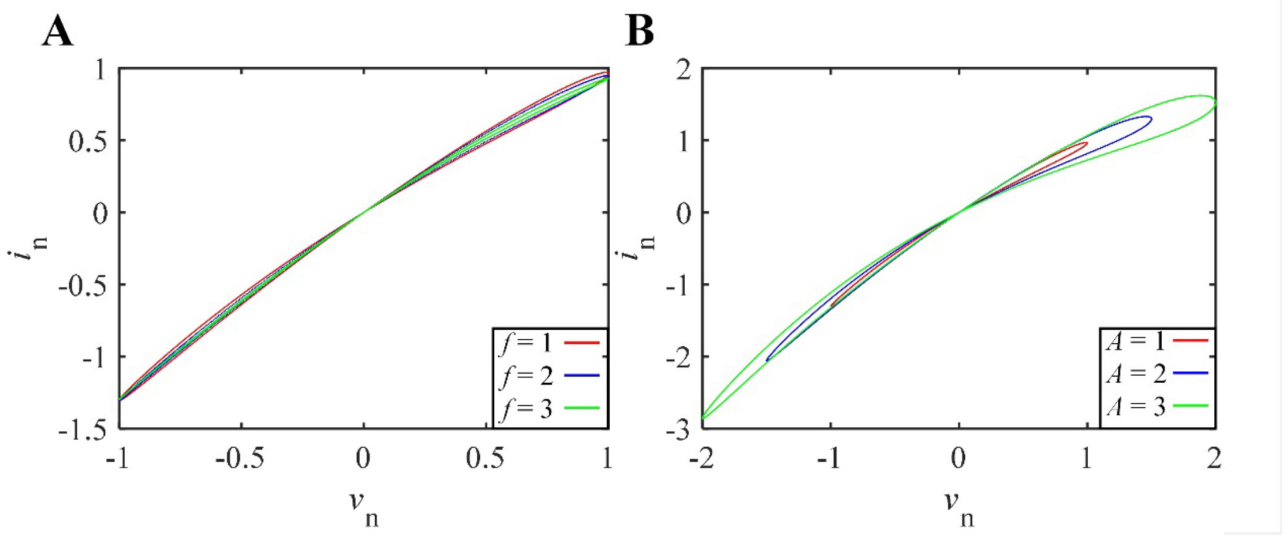

Figure 2. The tight hysteresis loop of the universal magnetically controlled memristor. (A) Pinched hysteresis loops with frequency variation; (B) Pinched hysteresis loops with amplitude variation.

aiming to simulate the electrical activity and synchronous behavior of biological neural systems. The mathematical model of the discrete tabu learning neuron model is shown in Equation (2). Where C denotes the membrane capacitance of the neuron, R denotes the membrane resistance of the neuron, W_{11} denotes the synaptic weight, α denotes the learning rate constant, and β denotes the memory decay rate constant. By self-coupling the universal magnetically controlled memristor proposed in this paper with a discrete tabu learning neuron, the TLNM model is constructed. The topology diagram of the TLNM model is shown in Figure 3.

$$\begin{cases} x\left(n+1\right) = -\frac{x(n)}{RC} + \frac{W_{11}T}{C}v_n + \frac{y(n)}{C} + \frac{I}{C} + x\left(n\right) \\ y\left(n+1\right) = -\alpha y\left(n\right) - \beta V + y\left(n\right) \end{cases} . \tag{2}$$

Let C = 1, I = 0, W_{11} = A, the mathematical model of the TLNM obtained by coupling the proposed universal magnetically controlled memristor with a discrete tabu learning neuron is shown in Equation (3).

$$\begin{cases} x\left(n+1\right) = -\frac{x(n)}{R} + AT\sin ax\left(n\right) + y\left(n\right) + x\left(n\right) \\ \quad +k\left(\tanh^3 z\left(n\right) + \tanh z\left(n\right)\right)x\left(n\right) \\ y\left(n+1\right) = -by\left(n\right) - cA\sin ax\left(n\right) + y\left(n\right) \\ z\left(n+1\right) = d\tanh\left(z^2(n) + z\left(n\right)\right) + ex\left(n\right) \end{cases} \tag{3}$$

3.2. Stability analysis

Through stability analysis, the structure of the attractor can be observed to a certain extent. To calculate the stable points of TLNM, let $x(n+1) = x(n), y(n+1) = y(n), z(n+1) = z(n)$, and the equilibrium equation obtained is shown in Equation (4).

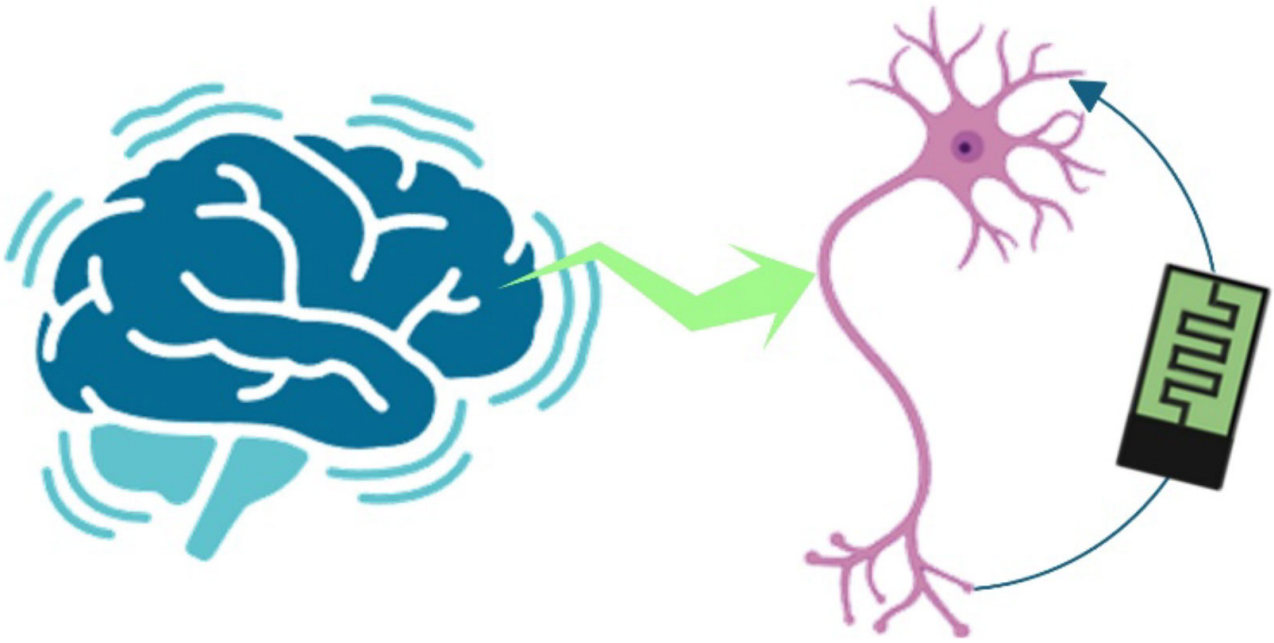

Figure 3. Topology of the tabu learning neuron-memristor model

$$\begin{cases} 0 = -\frac{x}{R} + AT\sin ax + y + k\left(\tanh^3 z + \tanh z\right)x \\ 0 = -by - cA\sin ax \\ 0 = d\tanh\left(z^2 + z\right) + ex - z \end{cases} \tag{4}$$

From the second equation of Equation (4), $y = -cA\sin ax/b$. Substituting this into the first equation simplifies Equation (4) to Equation (5).

$$\begin{cases} 0 = -\frac{x}{R} + AT\sin ax - \frac{cA}{b}\sin ax + k\left(\tanh^3 z + \tanh z\right)x \\ 0 = d\tanh\left(z^2 + z\right) + ex - z \end{cases} \tag{5}$$

Let $F_1(x,z) = -x/R + AT\sin ax - (cA\sin ax)/b + k(\tanh^3 z + \tanh z)x, F_2(x,z) = d\tanh(z^2 + z) + ex - z$. This allows us to transform the solution of Equation (5) into plotting the functions $F_1(x,z)$ and $F_2(x,z)$. The intersection point of these two functions is the equilibrium point. When $a = \pi$; $b = 1.6; c = 1.9; d = 1; e = 0.2; A = 0.5; T = 0.1; R = 0.6$; and $k = 0.6$, The graphs of functions $F_1(x,z)$ and $F_2(x,z)$ are shown in Figure 4A. It can be observed that there are two intersection points, indicating that the TLNM model has two equilibrium points under these parameters. When $a = \pi; b = 1.6; c = 1.9; d = 1; e = 0.2; A = 0.5; T = 0.1; R = 1$; and $k = 0.6$, The graphs of functions $F_1(x,z)$ and $F_2(x,z)$ are shown in Figure 4B. At this point, there are 11 intersection points, indicating that the TLNM model possesses 11 equilibrium points.

The Jacobian matrix for Equation (4) is shown in Equation (6).

$$\begin{bmatrix} k\left(\tanh^3 z + \tanh z\right) - \frac{1}{R} + ATa\cos ax & 1 & -kx\left(\tanh z^2 + 3\tanh z^2\left(\tanh z^2 - 1\right) - 1\right) \\ -Aac\cos ax & -b & 0 \\ e & 0 & -d\left(2z+1\right)\left(\tanh\left(z^2+z\right)^2 - 1\right) \end{bmatrix}. \tag{6}$$

The characteristic equation of this Jacobian matrix is given by Equation (7).

$$\lambda^3 - (\alpha + 2\theta)\lambda^2 + (\theta + 2\alpha\theta - \gamma + e)\lambda - \alpha\theta^2 + \gamma\theta - e\theta = 0. \tag{7}$$

where $\alpha = k(\tanh^3 z + \tanh z) - 1/R + ATa\cos ax; \beta = -kx(\tanh z^2 + 3\tanh z^2(\tanh z^2 - 1) - 1); \gamma = -Aac\cos ax; \theta = -d(2z + 1)(\tanh^2 z^2 + z)^2 - 1)$. Substituting the intersection coordinates from Figure 4A into Equation (7) yields the corresponding eigenvalues. The eigenvalues corresponding to $A_1(0,0)$ are $\lambda_1 = 0$, $\lambda_2 = -1.5548 + 1.727$i, $\lambda_3 = -1.5548 - 1.727$i (note that $A_1(0,0)$ is non-hyperbolic equilibrium point). The eigenvalue corresponding to $A_2(0.09858, 0.9791)$ is $\lambda_1 = -0.7635$, $\lambda_2 = -1.4705 + 1.6801$i, $\lambda_3 = -1.4705 - 1.6801$i (note that $A_2(0.09858, 0.9791)$ is unstable saddle focus).

4. The effect of parameters on the tabu learning neuron-memristor system

4.1. Effect of coupling parameter

To more clearly observe the effect of parameter k on the TLNM system, let $a = \pi$; $b = 1.6$; $c = 1.9$; $d = 1$; $e = 0.2$; $A = 0.5$; $T = 0.1$; and $R = 0.6$. The Lyapunov exponent spectrum and bifurcation diagram for parameter k varying over the interval $[0, 1]$ are depicted in Figure 5.[36] From the Lyapunov exponent spectrum, it can be observed that the TLNM system initially exhibits a hyperchaotic state. After a brief period, the system transitions into a chaotic state and subsequently enters a transient periodic state. Finally, after several brief cycles and chaotic states, the TLNM system returned to the hyperchaotic state as shown in Figure 5A. The bifurcation diagram in Figure 5B shows the variation in the x-sequence range of the TLNM system as the parameter k changes.

The coupling parameter k is selected for three different states based on the Lyapunov exponent spectrum. The plots for the corresponding attractors are shown in Figure 6. The attractor in the hyperchaotic, periodic, and chaotic states is shown in Figure 6A–6C. It can be observed that attractors in hyperchaotic states exhibit more complex structures than those in other states.

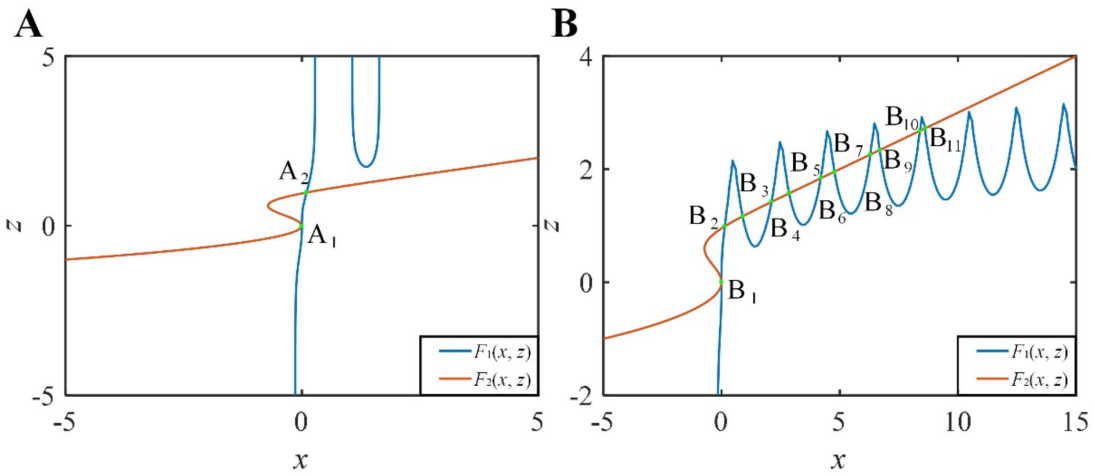

Figure 4. The graphs of functions $F_1(x, z)$and$F_2(x, z)$.(A)R = 0.6; (B) $R = 1$.

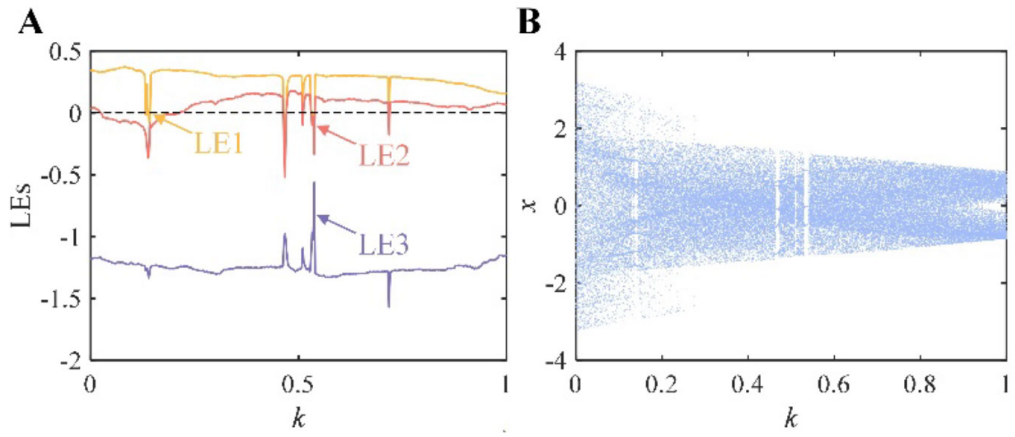

Figure 5. Lyapunov exponent spectrum and bifurcation diagram as a function of coupling parameter k. (A) Lyapunov exponent spectrum; (B) Bifurcation diagram.
Abbreviation: LE: Lyapunov exponent.

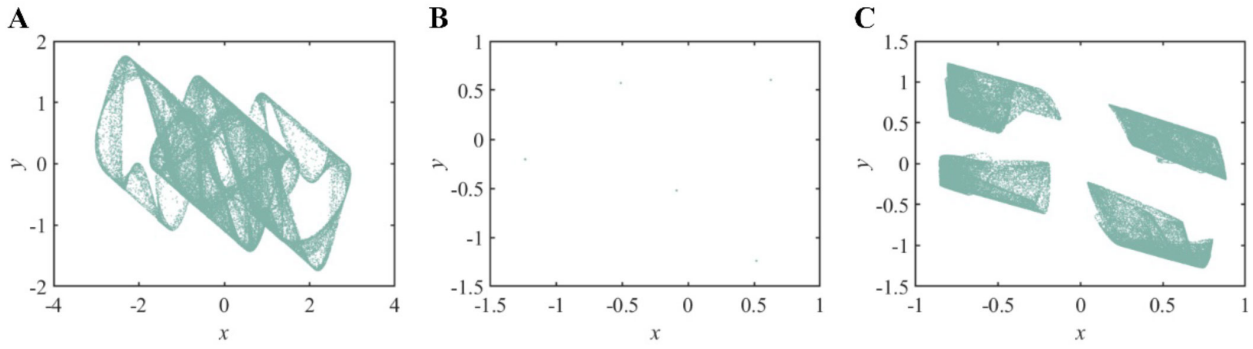

Figure 6. Attractors as a function of coupling parameter k. (A) k = 0.1 (hyperchaotic state); (B) k = 0.4675 (periodic state); (C) k = 1 (chaotic state).

4.2. Effect of memristor parameter d on the tabu learning neuron-memristor system

It is essential to investigate the impact of memristor parameter variations on the TLNM system. This section analyzes the memristor parameter d by plotting the Lyapunov exponent spectrum and bifurcation diagram as d varies over the interval $[0, 2]$, as shown in Figure 7. As the memristor parameter d increases, the TLNM system transitions from a chaotic state to a transient periodic state, then returns to a chaotic state. At d = 0.83, the TLNM system enters a hyperchaotic state. As d gradually increases to around 0.915, the TLNM system re-enters a transient periodic state before remaining in a hyperchaotic state thereafter, as shown in Figure 7A. From the bifurcation diagram as a function of memristor parameter d, it can be observed that the distributions of the x-sequence in the hyperchaotic state and the chaotic state are completely different, as shown in Figure 7B.

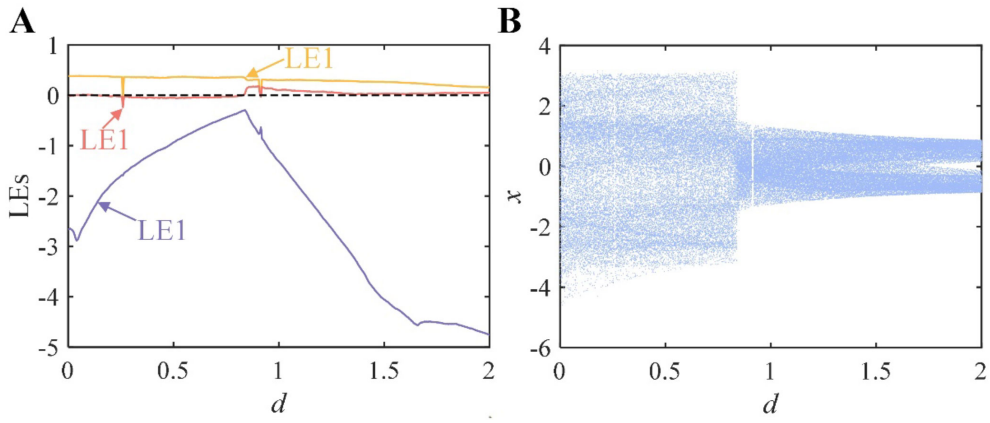

Figure 7. Lyapunov exponent spectrum and bifurcation diagram as the memristor parameter d varies. (A) Lyapunov exponent spectrum; (B) Bifurcation diagram
Abbreviation: LE: Lyapunov exponent.

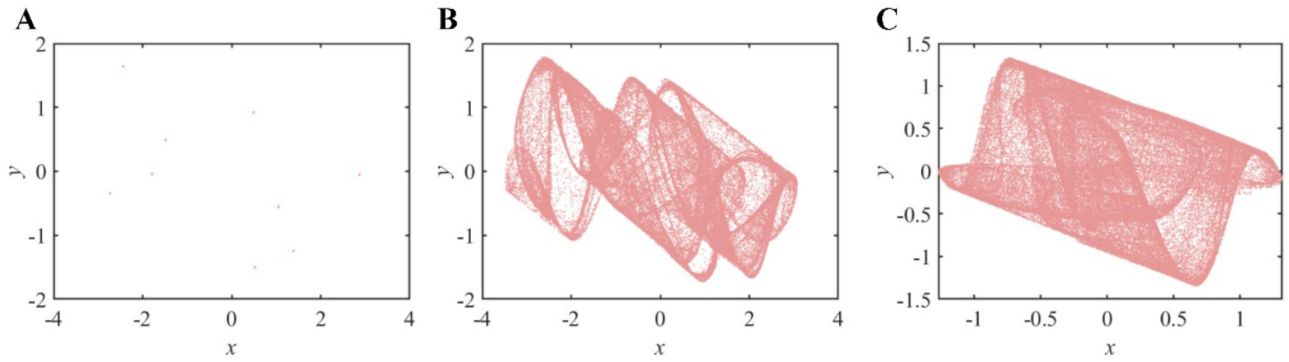

Figure 8. Attractors as a function of memristor parameter d. (A) d = 0.26; (B) d = 0.5. (C) d = 1.

The attractors in periodic, chaotic, and hyperchaotic states are depicted in Figure 8. The periodic, chaotic, and hyperchaotic attractors are shown in Figure 8A–8C (d = 0.26, d = 0.5, and d = 1, respectively).

4.3. Firing behavior of the tabu learning neuron-memristor system

All functions of the brain—thinking, memory, emotion, perception—stem from the complex network activity of approximately one hundred billion neurons communicating through electrical impulses (action potentials) and chemical signals. Therefore, it is necessary to study the firing behavior of the TLNM system. This section investigates the different firing behaviors exhibited by the TLNM system under various parameter R values, as shown in Figure 9. Let $a = \pi$; b = 1.6; c = 1.9; d = 1; e = 0.2; A = 0.5; T = 0.1; and k = 0.6, the chaotic, hyperchaotic, and periodic discharge pattern diagram as parameter R varies is shown in Figure 9A–9C.

4.4. Coexistence behavior of the tabu learning neuron-memristor system

The TLNM system is highly sensitive to initial conditions. Even slight variations in initial values can alter the system's attractors and discharge patterns. This section primarily investigates the coexistence behavior of the TLNM system. Let $a = \pi$; b = 1.6; c = 1.9; d = 1; e = 0.2; T = 0.1; R = 2.9; and k = 0.1, when plotting with initial values (2, −0.2, −0.2) and (−1, −0.2, −0.2), the coexistence bifurcation diagram as a function of parameter A is shown in Figure 10A. It can be observed that for $A \in [-0.6, 0.6]$, the TLNM system exhibits entirely different dynamical characteristics under different initial conditions. The coexisting attractors as A varies are shown in Figure 10. Chaos and periodicity coexisting attractors are shown in Figure 10B; chaos and chaos coexisting attractors are shown in Figure 10C; and periodicity and periodicity coexisting attractors are shown in Figure 10D.

4.5. Multi-cavity control of the tabu learning neuron-memristor system

Multi-cavity control has emerged as an important research focus in current chaos theory. Future brain–computer interfaces may not rely on single electrodes but instead utilize multidimensional electrode arrays. Multi-cavity control strategies enable precise intervention in neural networks to treat medical conditions, such as Parkinson's disease and epilepsy, while minimizing disruption to normal brain function. Therefore, it is essential to study multi-cavity control. This section employs a multi-level step function, as shown in Equation (8) for multi-cavity control.

$$\eta(\xi) = \sum_{\sigma=1}^{N} [(\xi + 2\sigma - 1) + (\xi - 2\sigma + 1)] \tag{8}$$

A multi-level step function is a signal whose value undergoes an instantaneous jump at specific time points and remains constant between jumps. It is essentially a linear combination of multiple fundamental unit step

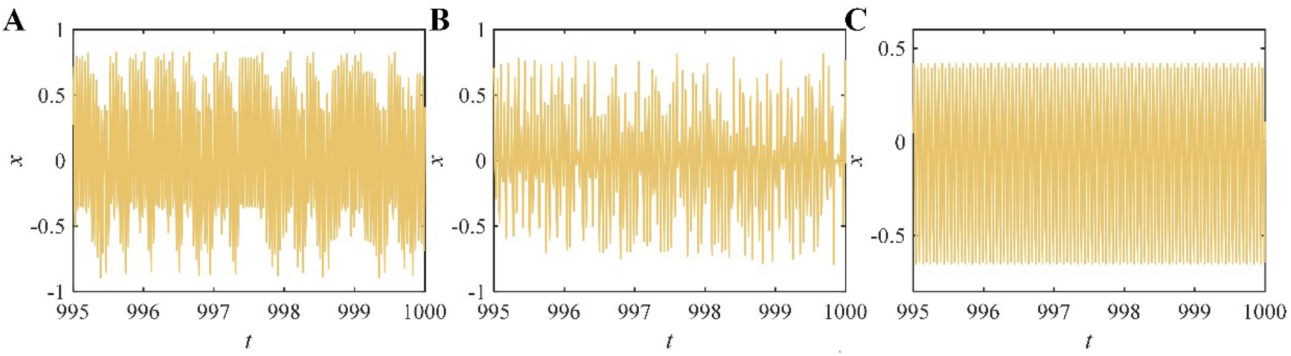

Figure 9. Firing behavior under different parameters R. (A) R = 1.3 (chaotic); (B) R = 2 (hyperchaotic); (C) R = 2.6 (periodic).

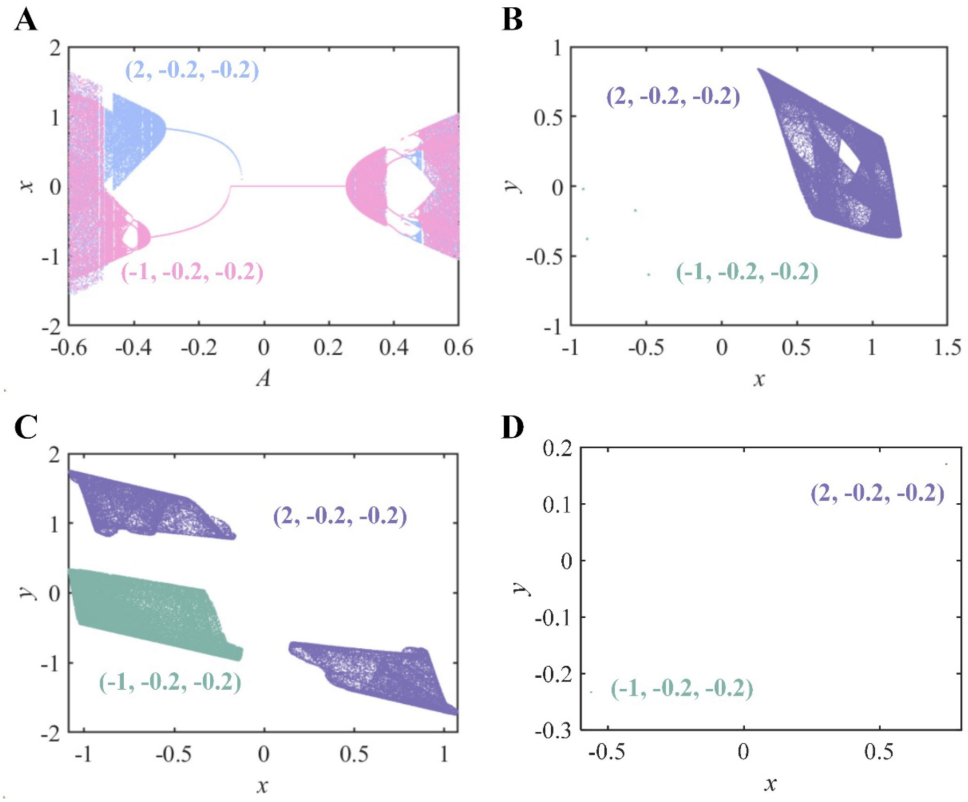

Figure 10. Coexistence phenomenon in the TLNM system. (A) Coexistence bifurcation diagram; (B) $A = -0.4$ (chaos and periodicity coexisting attractors); (C) $A = -0.4725$ (Chaos and chaos coexisting attractors); (D) $A = -0.2$ (Periodicity and periodicity coexisting attractors).

functions. It is also an exceptionally powerful and intuitive tool for modeling and analyzing various segmented constant processes in the real world, playing a crucial role in fields such as control engineering, signal processing, and system modeling. By incorporating this multi-level step function into Equation (3), a new system equation is constructed, as shown in Equation (9).

$$\begin{cases} x(n+1) = -\frac{x(n)}{R} + AT\sin ax(n) + y(n) + x(n) \\ \quad +k\left(\tanh^3 z(n) + \tanh z(n)\right)x(n) \\ y(n+1) = -by(n) - cA\sin ax(n) + y(n) \\ z(n+1) = d\tanh\left(z^2(n) + z(n)\right) + ex(n) \\ o(n+1) = \sum_{\sigma=1}^{N}\left[(o(n) + 2\sigma - 1) + (o(n) - 2\sigma + 1)\right] + \theta_1 x(n) \\ p(n+1) = \sum_{\sigma=1}^{N}\left[(p(n) + 2\sigma - 1) + (p(n) - 2\sigma + 1)\right] + \theta_2 x(n) \end{cases} \tag{9}$$

Let $a = \pi$; $b = 1.6$; $c = 1.9$; $d = 1$; $e = 0.2$; $A = 0.5$; $T = 0.1$; R = 1.6; $k = 0.1$; $\theta_1 = 1$; and $\theta_2 = 0.5$, with initial values (-0.4, -0.1, -0.1, o_0, -3). The bifurcation of initial values as o_0 varies is illustrated in Figure 11. As shown in the figure, the bifurcation diagram exhibits a stepwise increase.

Plots of 3 × 3 and 4 × 4 multi-cavity attractors were generated for N = 2 and N = 3, respectively (Figure 12). As shown in the figure, the attractor has undergone only a translational shift; its shape and structure remain unchanged. The complexity and interference resistance of chaotic sequences are enhanced through multi-cavity control, and their application in the secure communications field can increase security.

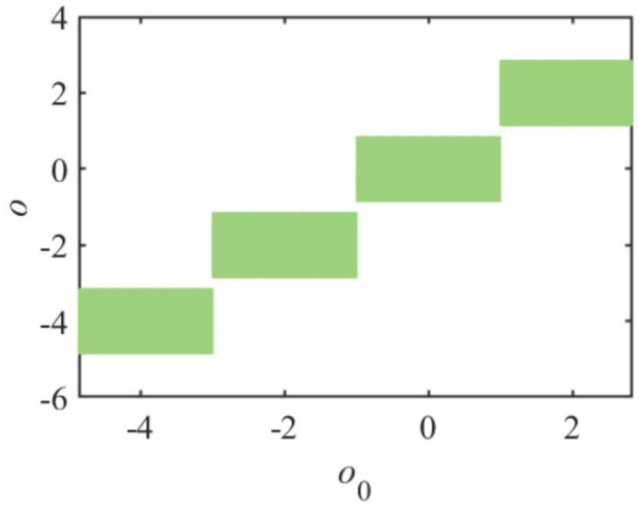

Figure 11. Initial value bifurcation diagram as the initial value o_0 increases

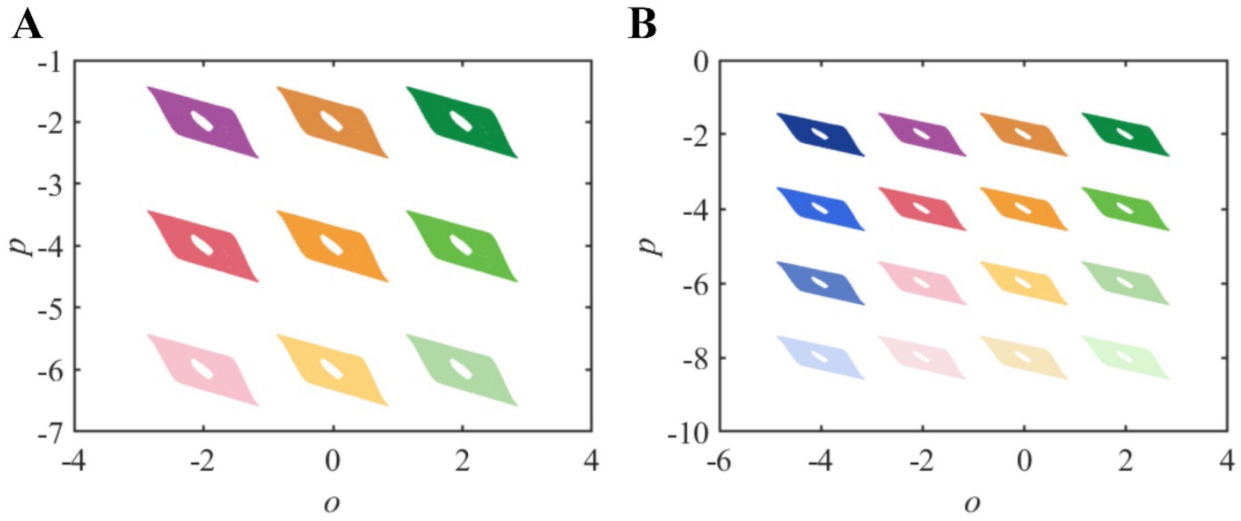

Figure 12. Multi-cavity attractors for different values of N. (A) $N = 2$; (B) $N = 3$.

4.6. Complexity of the tabu learning neuron-memristor system

Complexity can assess the randomness of chaotic sequences in a chaotic system, making complexity analysis essential. This section focuses on evaluating the spectral entropy complexity of the TLNM system. The SE complexity is derived through Fourier transforms and Shannon entropy. The closer the system's SE complexity approaches 1, the closer its chaotic sequence approximates a random sequence. Let $a = \pi$; $b = 1.6$; $c = 1.9$; $d = 1$; $e = 0.2$; $A = -0.2$; $T = 0.1$; and $R = 0.6$, the complexity of the TLNM system as a function of parameter k and initial value x is plotted with initial values (x, -0.1, -0.1), as shown in Figure 13A and 13C. It can be observed that under these parameters, the complexity of the TLNM system approaches 1. Let $a = \pi$; $b = 1.6$; $c = 1.9$; $d = 1$; $e = 0.2$; $A = -0.2$; $T = 0.1$; and $k = 0.6$, the initial values (x, -0.1, -0.1) are plotted to illustrate the complexity of the TLNM system as parameters R and initial value x vary, as shown in Figure 13B and 13D. It can be observed that under these parameters, the complexity of the TLNM system also approaches 1. This demonstrates that the chaotic sequences generated by the TLNM system exhibit high randomness, making them suitable for the secure communications field.[37–39]

5. Demand-side platform implementation

To verify the physical feasibility of the TLNM system, this paper implements its attractor using a DSP. DSP features high real-time performance, computational efficiency, energy efficiency, integration density, and stability, making them well-suited for verifying the physical feasibility of the TLNM system. The hardware and steps for DSP implementation are shown in Figure 14. The TMS320F28335 chip generates chaotic signals, which are then converted into analog signals via a digital-to-analog converter. Finally, the attractor is visualized through a filter.

This section investigates the effect of the same parameters and initial conditions shown in Figure 8C on achieving the same attractor through DSP implementation, as shown in Figure 15. The DSP setup and the resulting presentation are shown in Figure 15A. Comparisons show that the results obtained with the DSP match those simulated in the paper, indicating that the chaotic signals generated using this neuron can be produced with a DSP.

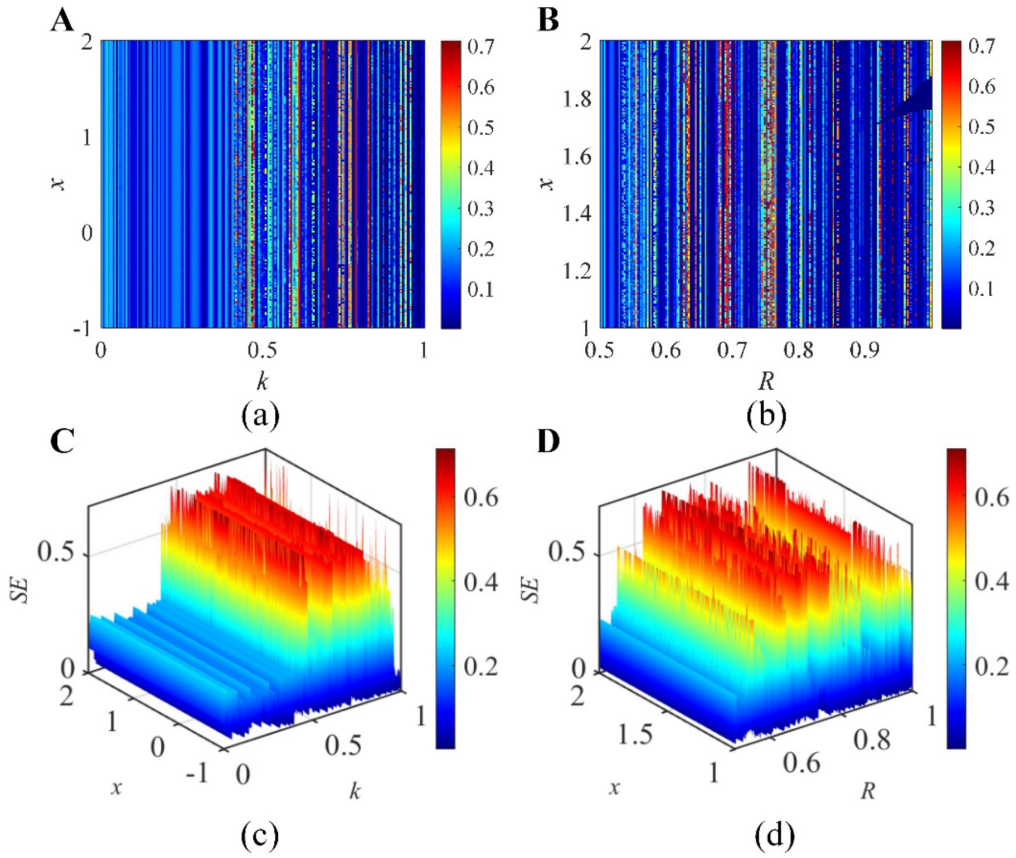

Figure 13. SE complexity of the tabu learning neuron-memristor system. (A) Complexity of the two-dimensional SE for sequence x and parameter k; (B) Complexity of the two-dimensional SE for sequence x and parameter R; (C) Complexity of the three-dimensional SE for sequence x and parameter k; (D) Complexity of the three-dimensional SE for sequence x and parameter R.
Abbreviation: SE: Spectral entropy.

Figure 14. DSP steps and connection diagram
Abbreviations: D/A: Digital-to-analog converter; DSP: Demand-side platform; SPI: Serial peripheral interface.

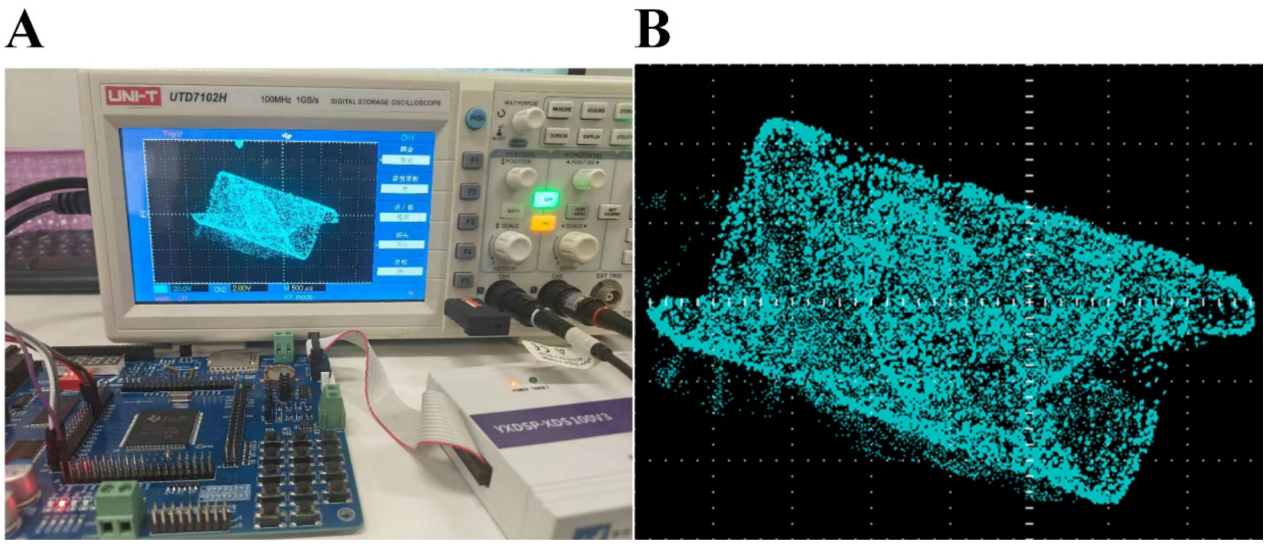

Figure 15. Experimental results of the demand-side platform (DSP). (A) Hardware setup of the DSP; (B) DSP presentation result.

6. Conclusion

This paper proposes a novel universal magnetically controlled memristor based on the tanh function's smooth, differentiable, and symmetric soft saturation. It is self-coupled with a discrete tabu learning neuron to construct the TLNM. Through computational analysis, the equilibrium points of the TLNM system are studied, revealing that the number of equilibrium points varies with parameter changes. Through numerical analysis, the effects of the coupling parameter k and the memristor parameter d on the system are investigated. As the coupling parameter k and the memristor parameter d vary, the TLNM system undergoes transitions between hyperchaotic, chaotic, and periodic states. After investigating the system parameter R, it was found that the system exhibited a wide range of firing behaviors. Under different initial conditions, the TLNM system exhibited coexisting attractors, revealing its multistability. By incorporating a multi-level step function into the TLNM system equations, multi-cavity control of the attractor was achieved. SE complexity analysis revealed that the chaotic sequences generated by the TLNM system were highly random. These chaotic sequences are well-suited for application in the secure communications field. The physical feasibility of the system was validated through the DSP. The TLNM system proposed in this paper provides a theoretical foundation for brain-inspired research.

Acknowledgments

None.

Funding

This work was supported by the Basic scientific research projects in department of education of Liaoning Province (Grant No. LJ212410152011), Doctoral Research Startup Fund Program Project of Liaoning Province (Grant No. 2025-BS-0471), Research startup fund project for introducing talents of Dalian Polytechnic University (Grant No. LJBKY2025070), Basic Scientific Research Projects in Department of Education of Liaoning Province (Grant No. LJ212410152049), and National Natural Science Foundation of China (Grant No. 62571079).

Conflict of interest

The authors declare that they have no competing interests.

Author contributions

Conceptualization: Suo Gao, Jun Mou
Investigation: Xianying Xu
Methodology: Xiaodong Liu
Writing–original draft: Yinghong Cao
Writing–review & editing: Xiyu Ren

Availability of data

Data used in this work is available from the corresponding author upon reasonable request.

AI Tools Statement

The authors confirm that no artificial intelligence (AI) tools were used in the preparation of this manuscript.

References

1. Swanson LW. What is the brain? *Trends in neurosciences.* 2000;23(11):519-527. https://doi.org/10.1016/S0166-2236(00)01639-8
2. Zeki S. Art and the brain. *Journal of Consciousness Studies.* 1999;6(6-7):76-96. https://doi.org/10.1017/cbo9781139030410.004
3. Boccaletti S, Grebogi C, Lai Y-C, Mancini H, Maza D. The control of chaos: theory and applications. *Physics reports.* 2000;329(3):103-197. https://doi.org/10.1016/s0370-1573(99)00096-4
4. Mahmoudvand S, Ghazavi MR, Farrokhabadi A. Nonlinear dynamic modeling and chaos analysis of aircraft landing gear under two-and three-point landings. *Nonlinear Science and Control Engineering.* 2025;1(1):025280001. https://doi.org/10.36922/NSCE025280001
5. Aihara K. Chaos engineering and its application to parallel distributed processing with chaotic neural networks. *Proceedings of the IEEE.* 2002;90(5):919-930. https://doi.org/10.1109/jproc.2002.1015014
6. Kadmon J, Sompolinsky H. Transition to chaos in random neuronal networks. *Physical Review X.* 2015;5(4):041030. https://doi.org/10.1103/PhysRevX.5.041030
7. Hodgkin AL, Huxley AF. A quantitative description of membrane current and its application to conduction and excitation in nerve. *The Journal of physiology.* 1952;117(4):500. https://doi.org/10.1113/jphysiol.1952.sp004764
8. Guo Z-H, Li Z-J, Wang M-J, Ma M-L. Hopf bifurcation and phase synchronization in memristor-coupled Hindmarsh–Rose and FitzHugh–Nagumo neurons with two time delays. *Chinese Physics B.* 2023;32(3):038701. https://doi.org/10.1088/1674-1056/aca601
9. Yang Y, Liao X. Filippov Hindmarsh–Rose neuronal model with threshold policy control. *IEEE transactions on neural networks and learning systems.* 2018;30(1):306-311. https://doi.org/10.1109/TNNLS.2018.2836386
10. Wu L, Yang S, Bai Y, Machado JM. Efficient robust optimization based on polynomial chaos and tabu search algorithm. *International Journal of Applied Electromagnetics and Mechanics.* 2012;39(1-4):145-150. https://doi.org/10.3233/jae-2012-1454
11. Njitacke ZT, Nkapkop JDD, Signing VF, Tsafack N, Sone ME, Awrejcewicz J. Novel extreme multistable tabu learning neuron: Circuit implementation and application to cryptography. *IEEE Transactions on Industrial Informatics.* 2022;19(8):8943-8952. https://doi.org/10.1109/TII.2022.3223233
12. Cao Z, Sun B, Zhou G, et al. Memristor-based neural networks: a bridge from device to artificial intelligence. *Nanoscale Horizons.* 2023;8(6):716-745. https://doi.org/10.1039/d2nh00536k
13. Zhang S, Wang C, Zhang H, Lin H. Collective dynamics of adaptive memristor synapse-cascaded neural networks based on energy flow. *Chaos, Solitons Fractals.* 2024;186:115191.
14. Deng W, Ma M. Analysis of the dynamical behavior of discrete memristor-coupled scale-free neural networks. *Chinese Journal of Physics.* 2024;91:966-976. https://doi.org/10.1016/j.cjph.2024.08.033
15. Li C, Li Y, Yu W, Moroz I, Volos C. Constructing conditional symmetry in a chaotic map. *Nonlinear Dynamics.* 2025;113(4):3857-3868. https://doi.org/10.1007/s11071-024-10368-6
16. Chua L. Memristor-the missing circuit element. *IEEE Transactions on circuit theory.* 2003;18(5):507-519. https://doi.org/10.1109/TCT.1971.1083337
17. Kim H, Sah MP, Yang C, Cho S, Chua LO. Memristor emulator for memristor circuit applications. *IEEE Transactions on Circuits and Systems I: Regular Papers.* 2012;59(10):2422-2431. https://doi.org/10.1109/TCSI.2012.2188957
18. Chanthbouala A, Garcia V, Cherifi RO, et al. A ferroelectric memristor. *Nature materials.* 2012;11(10):860-864. https://doi.org/10.1038/nmat3415

19. Ascoli A, Corinto F, Senger V, Tetzlaff R. Memristor model comparison. *IEEE Circuits and Systems Magazine.* 2013;13(2):89-105. https://doi.org/10.1109/MCAS.2013.2256272
20. Jeong H, Shi L. Memristor devices for neural networks. *Journal of Physics D: Applied Physics.* 2018;52(2):023003. https://doi.org/10.1088/1361-6463/aae223
21. Duan H, Cheng S, Qin L, et al. Low-power memristor based on two-dimensional materials. *The Journal of Physical Chemistry Letters.* 2022;13(31):7130-7138. https://doi.org/10.1021/acs.jpclett.2c01962
22. Wan Z, Pu Y-F, Lai Q. Memristive feedback-controlled chaotic system with diverse dynamics. *Nonlinear Science and Control Engineering.* 2025;1(1):025310008. https://doi.org/10.36922/NSCE025310008
23. Li J, Wang C, Deng Q. Symmetric multi-double-scroll attractors in Hopfield neural network under pulse controlled memristor. *Nonlinear Dynamics.* 2024;112(16):14463-14477. https://doi.org/10.1007/s11071-024-09791-6
24. Li C, Yang Y, Yang X, Zi X, Xiao F. A tristable locally active memristor and its application in Hopfield neural network. *Nonlinear Dynamics.* 2022;108(2):1697-1717. https://doi.org/10.1007/s11071-022-07268-y
25. Chen Q, Li B, Yin W, Jiang X, Chen X. Bifurcation, chaos and fixed-time synchronization of memristor cellular neural networks. *Chaos, Solitons Fractals.* 2023;171:113440. https://doi.org/10.1016/j.chaos.2023.113440
26. Yang F, Ma J, Wu F. Review on memristor application in neural circuit and network. *Chaos, Solitons Fractals.* 2024;187:115361. https://doi.org/10.1016/j.chaos.2024.115361
27. Lai Q, Yang L. Discrete memristor applied to construct neural networks with homogeneous and heterogeneous coexisting attractors. *Chaos, Solitons & Fractals.* 2023;174:113807. https://doi.org/10.1016/j.chaos.2023.113807
28. Yu F, Kong X, Yao W, et al. Dynamics analysis, synchronization and FPGA implementation of multiscroll Hopfield neural networks with non-polynomial memristor. *Chaos, Solitons & Fractals.* 2024;179:114440. https://doi.org/10.1016/j.chaos.2023.114440
29. Lu J, Xie X, Lu Y, Wu Y, Li C, Ma M. Dynamical behaviors in discrete memristor-coupled small-world neuronal networks. *Chinese Physics B.* 2024;33(4):048701. https://doi.org/10.1088/1674-1056/ad1483
30. Ding S, Wang N, Bao H, Chen B, Wu H, Xu Q. Memristor synapse-coupled piecewise-linear simplified Hopfield neural network: Dynamics analysis and circuit implementation. *Chaos, Solitons & Fractals.* 2023;166:112899. https://doi.org/10.1016/j.chaos.2022.112899
31. Shang C, He S, Rajagopal K, Wang H, Sun K. Dynamics and chimera state in a neural network with discrete memristor coupling. *The European Physical Journal Special Topics.* 2022;231(22):4065-4076. https://doi.org/10.1140/epjs/s11734-022-00699-z
32. Ren X, Xu X, Al-Barakati AA, Cao Y. Emotional changes induced by associative memory. *The European Physical Journal Special Topics.* 2025:1-11. https://doi.org/10.1140/epjs/s11734-025-01654-4
33. Mou J, Cao H, Zhou N, Cao Y. An FHN-HR neuron network coupled with a novel locally active memristor and its DSP implementation. *IEEE Transactions on Cybernetics.* 2024;54(12):7333-7342. https://doi.org/10.1109/TCYB.2024.3471644
34. Lin H, Wang C, Sun J, Zhang X, Sun Y, Iu HH. Memristor-coupled asymmetric neural networks: Bionic modeling, chaotic dynamics analysis and encryption application. *Chaos, Solitons & Fractals.* 2023;166:112905. https://doi.org/10.1016/j.chaos.2022.112905
35. Zhang J, Bao H, Gu J, Chen M, Bao B. Multistability and synchronicity of memristor coupled adaptive synaptic neuronal network. *Chaos, Solitons & Fractals.* 2024;185:115157. https://doi.org/10.1016/j.chaos.2024.115157
36. Shimada I, Nagashima T. A numerical approach to ergodic problem of dissipative dynamical systems. *Progress of theoretical physics.* 1979;61(6):1605-1616. https://doi.org/10.1143/PTP.61.1605
37. Mou J, Tan L, Cao Y, Zhou N, Zhang Y. Multi-face image compression encryption scheme combining extraction with STP-CS for face database. *IEEE Internet of Things Journal.* 2025;12(12):19522-19531. https://doi.org/10.1109/JIOT.2025.3541228
38. Tan L, Cao Y, Banerjee S, Mou J. Multi-medical image protection: compression–encryption scheme based on tlnn and mask cubes. *The Journal of Supercomputing.* 2025;81(1):96. https://doi.org/10.1007/s11227-024-06624-6
39. Mou J, Zhang Z, Banerjee S, Zhang Y. Combining semi-tensor product compressed sensing and session keys for low-cost encryption of batch information in WBANs. *IEEE Internet of Things Journal.* 2024;11(20):33565-33576. https://doi.org/10.1109/JIOT.2024.3429349